Institute of Space and Aeronautical Science, University of Tokyo
Report No. 465, June 1971

Development of 18% Nickel Maraging Steel Rocket Motor Cases

By

Daikichiro MORI, Yoshio ANDO*, Kazuhisa SUZUKI**
and Akira NAKANO

Summary: Development of 18% Ni maraging steel for rocket motor cases during the past six years is reported. The fundamental research on strength, ductility, notch toughness of both the base material and welds are described. Results of hydrostatic tests of the model vessels to establish the structural integrity and to verify adequacy of the material selection, fabrication techniques and heat-treatment methods are described, and finally the application to Mu and Lambda rocket motor cases are briefly reported.

1. INTRODUCTION

Design of Lambda and Mu rocket vehicle at the Institute of Space and Aeronautical Science, University of Tokyo required high performance motor cases.

As the candidate material for these new motor cases, maraging steel was selected and extensive researches including material selection, welding techniques, heat treating method, burst test of model vessels and static firing of the engine were undertaken.

In July 1964, PH 200, that is 18% Ni-9Co-5Mo maraging steel, was applied for the first time to the third stage motor case (diameter 420 mm) of the Lambda-3 rocket.

Since then, it has been used for the third stage motor case (diameter 500 mm) of Lambda-3H and -4S rockets.

Further research was performed to apply PH 200 to the first stage, the second stage (diameter 1400 mm) and the third stage motor cases (diameter 860 mm) of the M-4S rocket and as a result, the flight test of the M-1-1 rocket was successfully conducted in October 1966.

In this report, the results of a series of basic research associated with the development of these motor cases such as heat treatment properties, strength, ductility, toughness, characteristics of weld and bursting properties of small models are explained.

* Professor, Faculty of Engineering, University of Tokyo.
** Kobe Technical Institute, Mitsubishi Heavy Industry Co., Ltd.

Table 1. Chemical composition of the tested maraging Steel (%)

Steel	Charge No.	Melting process	Plate thickness mm	C	Si	Mn	P	S	Ni	Co	Mo	Ti	Al	Zr	B	The date of production
A	——	V. M.	1.0	.03	.08	.08	.003	.020	17.57	8.62	4.56	.42	.065	.53	.004	Jan. 1967
B-1	——	A. M.	2.8	.024	.07	.07	.003	.004	18.33	9.30	5.06	.82	.074	.001	.003	Feb. 1963
B-2	——	V. M.	2.8	.02	.03	.04	.003	.003	18.17	9.32	4.81	.69	.097	.008		Apr. 1963
C	——	A. M.	5.0	.024	.07	.07	.003	.004	18.33	9.30	5.06	.82	.074	.001	.003	Feb. 1963
D	K4-7008	A. M.	1.7	.022	.10	.08	.013	.007	17.21	8.93	4.78	.77	.17	.001	.003	——
E-1	K29115(PS573)	A. M.	6.0	.019	.10	.04	.005	.007	18.78	9.22	4.98	.77	.19	.015	.003	——
E-2	K29116(PS574)			.034	.08	.05	.005	.006	17.91	8.34	4.96	.76	.17	.010	.003	——
F	43.96	A. M.	15.0	.020	.08	.04	.004	.016	18.43	8.65	5.00	.34	.038	.008	.004	Apr. 1965
G	(5F6911A)	V· M.	13.0	.020	.16	.05	.001	.014	18.01	8.85	4.80	.37	.095	.008	.0032	Apr. 1965
H	K2-9205(5F8758)	A. M.	10.0	.013	.03	.01	.002	.015	18.77	8.30	3.07	.18	.060	.010	.0025	Apr. 1965
I	K2-9206(5F8756)	A. M.	10.0	.014	.03	.03	.003	.014	18.68	7.83	4.84	.20	.100	.017	.0022	Apr. 1965
J	43-9684(5G4724)	V. M.	10.0	.029	.09	.07	.003	.019	17.52	8.63	4.57	.43	.070	.041	.0035	May. 1965
K	K2-9207(5F8757)	A. M.	10.0	.012	.04	.01	.002	.013	19.42	8.74	4.75	.70	.110	.015	.0009	Apr. 1965
L	K4-7480(5H6226)	V. M.	10.0	.020	.10	.04	.004	.013	18.75	8.73	4.80	.57	.100	.014	.003	Jun. 1965
M	——	V. M.	11.0	.023	.06	.025	.003	.014	18.80	8.84	5.20	.71	.100	.043	.0028	Oct. 1968

A. M.: Air melt material
V. M.: Vacuum melt material

Table 2. Physical and Metallurgical properties

Steel	Transformation Point (°C)				Coefficient of thermal expansion [°C^{-1} (0~500°C)]	Young's modulus (Kg/mm^2)	Specific gravity (g/cm^3)
	Ac1	Ac3	Ms	Mf			
H	—	—	—	—	—	1.86×10^4	8.07
L	530	640	160	100	10.0×10^{-6}	1.86×10^4	8.08

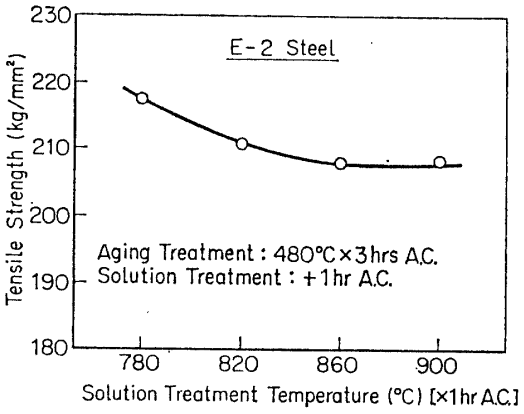

FIG. 1. Effect of solution treatment temperature on tensile strength.

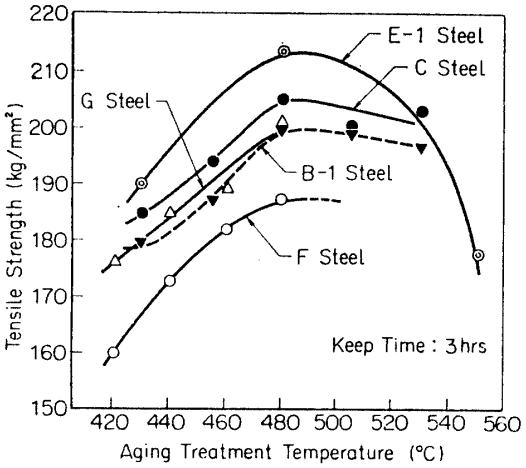

FIG. 2. Effect of aging treatment temperature on tensile strength.

2. CHARACTERISTICS OF BASE METAL

2-1 Chemical composition

The chemical composition of the tested maraging steels is the 18% Ni-9% Mo type, which is shown in Table 1. These steels were made by Kawasaki Steel Works. Only H Steel is made of 3% Mo in order to reduce its strength.

2-2 Physical and metallurgical properties

Transformation point of maraging steel, coefficient of thermal expansion, Young's modulus, specific gravity and other physical and metallurgical properties are shown in Table 2. The transformation point and coefficient of thermal expansion were measured by heating and cooling (rate: 180°C/hr) a 5 mm diameter 80 mm long test specimen. Young's modulus was obtained from the stress-strain relationship measured by tensile specimen fabricated through standard heat treatment.

2-3 Heat treatment characteristics

Heat treatment of maraging steels is a solution heat treatment after roll and subsequent aging process. The strength of the steel depends deeply on conditions of aging. Figure 1 shows the relationship between tensile strength and temperature of the solution treatment. After the solution treatment, the steel was aged at 480°C for 3 hrs and cooled in air.

Table 3. Results of the tensile test

Steel	Melting process	Plate thickness (mm)	Aging treatment	Roll dir.	Strength (Kg/mm²) Yield	Strength (Kg/mm²) Tensile	Elongation in 50mm (%)	Yield ratio
A	V.M.	1.0	480°C×3hrsA.C.	L	170.2	176.1	2.2	.97
					169.4	174.5	2.5	.97
				C	170.2	173.6	GL=25mm 0	.98
					169.7	172.6	0	.98
B-1	A.M.	2.8	480°C×3hrsA.C.	L	—	200.0	6.0	—
B-2	V.M.	2.8	480°C×3hrsA.C.	L	—	201.0	5.0	—
C	A.M.	5.0	480°C×3hrsA.C.	L	—	209.5	6.5	—
						211.1	5.0	
					199.1	205.0	7.5	.97
				C	202.2	207.0	5.0	.98
D	A.M.	1.7	480°C×3hrsA.C.	L	192.0	194.5	4.5	.99
					189.2	193.3	4.5	.98
				C	193.3	198.6	4.0	.97
					194.8	199.0	4.0	.98
E-1	A.M.	6.0	480°C×3hrsA.C.	L	205.0	212.0	5.5	.97
					205.1	214.4	5.5	.96
F	A.M.	15.0	480°C×3hrsA.C.	L	185.0	187.1	12.5	.99
					183.8	187.4	13.0	.98
		15→5	480°C×3hrsA.C.	L	183.0	185.9	8.0	.99
					180.5	184.2	8.0	.98
G	V.M.	13.0	480°C×3hrsA.C.	L	192.0	200.0	9.0	.96
				C	—	206.0	8.0	—
		13→5	450°C×3hrsA.C.	L	—	186.5	7.0	—
						185.6	7.0	
H	A.M.	10.0	480°C×3hrsA.C.	L	137.0	140.0	14.0	.98
				C	142.0	147.0	11.0	.97
		10→5	480°C×3hrsA.C.	L	136.0	140.8	8.5	.97
					135.0	140.8	9.5	.96
I	A.M.	10.0	450°C×3hrsA.C.	L	172.0	179.0	11.0	.96
				C	170.0	181.0	11.0	.94
		10→5	450°C×3hrsA.C.	L	167.0	170.2	8.5	.98
					167.0	170.6	9.0	.98

Table 3. (Continued)

Steel	Melting process	Plate thickness (mm)	Aging treatment	Roll dir.	Strength (Kg/mm²) Yield	Strength (Kg/mm²) Tensile	Elongation in 50 mm (%)	Yield ratio
J	V. M.	10.0	440°C×3hrsA.C.	L	160.0	173.0	11.0	.93
				C	162.1	176.0	10.0	.92
		10→5	440°C×3hrsA.C.	L	169.0	171.8	8.0	.98
					168.0	171.8	8.5	.98
K	A. M.	10.0	450°C×3hrsA.C.	L	191.0	204.0	9.0	.94
				C	203.0	214.0	6.0	.95
		10→5	450°C×3hrsA.C.	L	190.0	195.4	7.0	.97
					190.0	195.4	7.0	.97
L	V. M.	10.0	480°C×3hrsA.C.	L	196.0	202.0	11.0	.97
				C	196.0	206.0	8.0	.95
		10→5	480°C×3hrsA.C.	L	188.1	192.7	6.5	.98
					187.0	190.6	6.5	.98
M	V. M.	11.0	480°C×3hrsA.C.	L	180.5	186.5	9.0	.97
					180.1	188.1	8.0	.96
				C	178.4	188.7	7.0	.95
					183.5	193.7	7.0	.95

AM: Air melt material.
VM: Vacuum melt material.

Table 4. Results of the ductility test

Steel	Strength (Kg/mm²) Yield	Strength (Kg/mm²) Tensile	General elongation (%)
H	137	139.2	2.17
I	161	163.7	1.02
J	150	158.1	1.83
K	195	203.0	1.06
L	190	197.1	1.02
M	180.3	187.3	1.05

Figure 2 shows the variation of tensile strength under the aging treatment in the temperature range of 420–530°C. Figure 3 shows the effect of aging time on tensile strength.

These figures show that the aging treatment at 480°C × 3 hrs followed by air

cooling gives the highest strength.

Further, it appears that the optimal heat treatment conditions for maraging steels in this series are solution treatment at 820°C × 1 hr with air cooling, and aging treatment at 480°C × 3 hrs with air cooling.

2-4 *Strength and ductility*

Table 3 shows the results of tensile tests of maraging steels.

The results of the ductility tests are listed in Table 4, which is obtained from the relation between the elongation and the ratio $\sqrt{A}/(\text{G.L.})$ (A=Sectional Area, G.L.=Gauge Length). In this connection, general elongation, denoted (a), corresponds to the elongation taking place when the gauge length is infinitely large.

The larger this value, the better the ductility of the material. The typical relation between yield strength (σ_y) and general elongation (a) is shown in Figure 4.

From this relationship, we obtained an experimental formula;

$$a=108.3/(\sigma_y-83.8).$$

Some examples of the tensile strength of maraging steels at high temperature are shown in Figure 5. It can be seen that the strength decreases linearly as the test temperature increases.

Consequently, in the design of rocket motor cases which will be used at high temperature environment, this decrease in strentgh must be taken into consideration.

2-5 *Fracture toughness*

The most important requirement for the pressure vessel of the high strength steel is a high notch toughness, and we made three types of fracture toughness tests. These were Charpy impact test, NASA notch tension test and ASTM notch tension test.

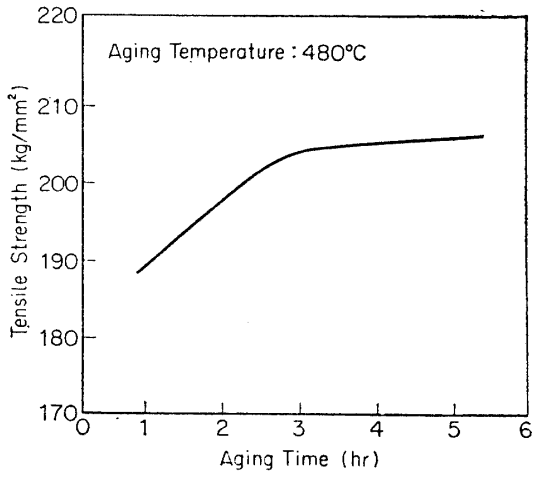

FIG. 3. Effect of aging time on tensile strength (B-1 steel).

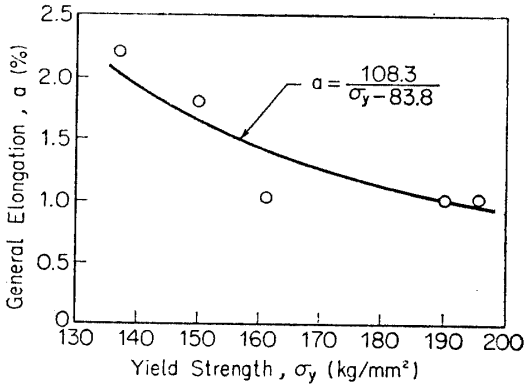

FIG. 4. Variation of yield strength with general elongation.

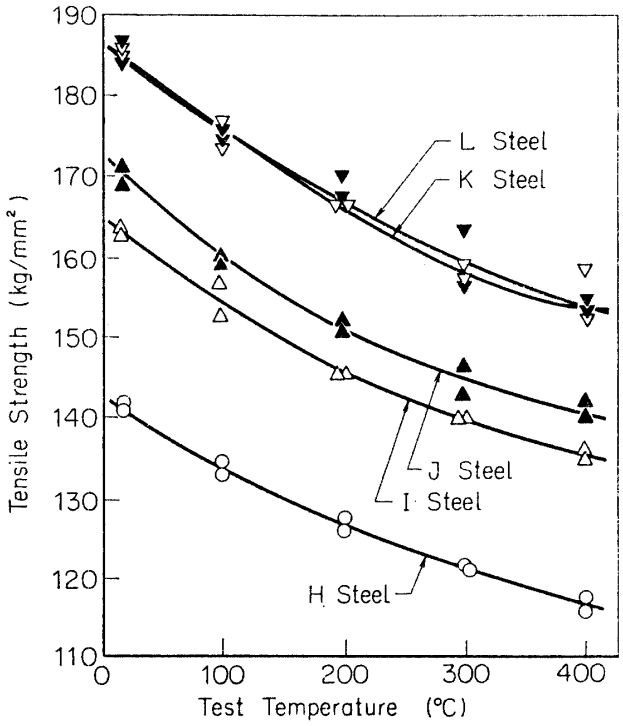

FIG. 5. Examples of the tensile strength of maraging steel at high temperature.

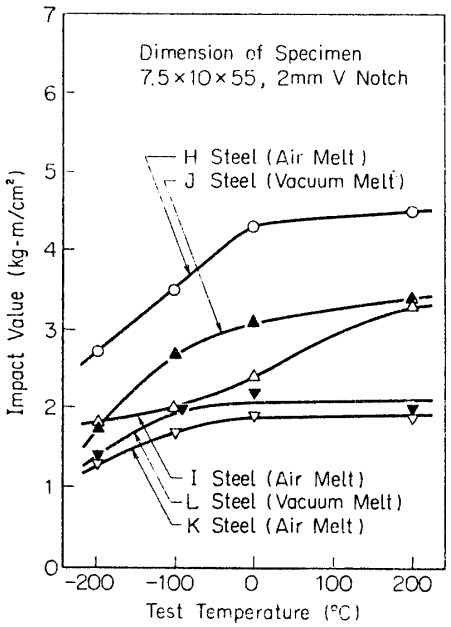

FIG. 6. Results of V-notch Charpy impact test of base metal (average of triplicate tests).

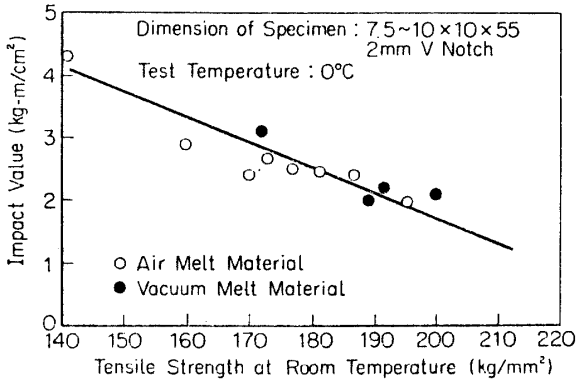

FIG. 7. Tensile strength at room temperature vs. impact valve.

1) Charpy impact test

Figure 6 shows the Charpy transition curves of some maraging steels under the various tensile strength levels and melting processes.

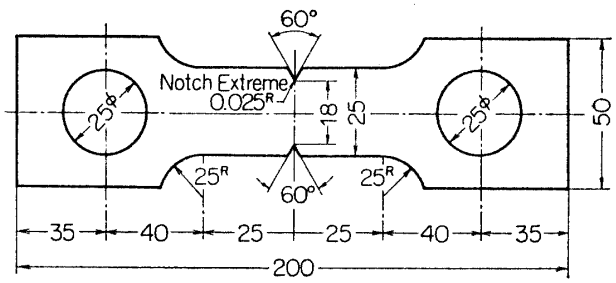

FIG. 8. Specimen of NASA notch tension test.

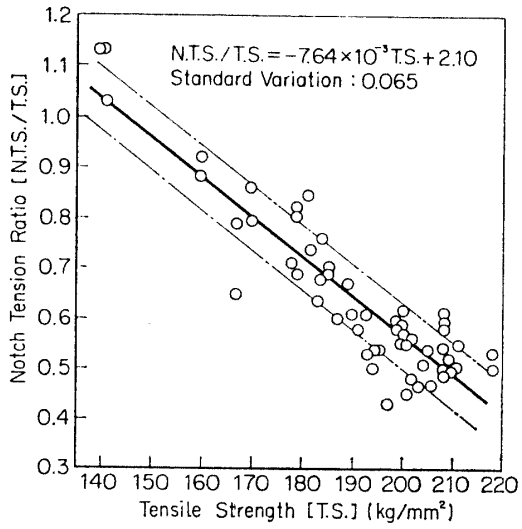

FIG. 9. Results of NASA notch tension test of the air melt materials.

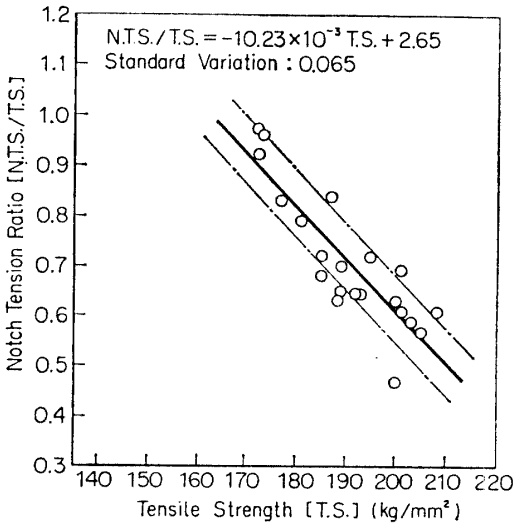

FIG. 10. Results of NASA notch tension test of the vacuum melt materials.

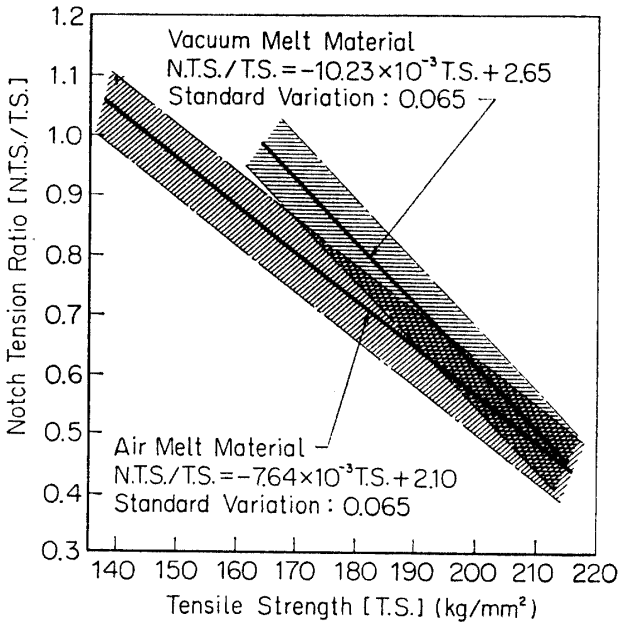

FIG. 11. Results of NASA notch tension test for the air melt materials and vacuum melt materials.

From these curves and Table 4, it is clear that the higher the strength level, the lower the Charpy impact value, and that for the same strength steels, the impact value of vacuum melted materials is higher than that of air melted materials.

The relationship between impact values at 0°C, which lies almost at the same level with those at room temperature, and tensile strength at room temperature is shown in Figure 7.

2) NASA notch tension test

NASA notch tension tests were carried out with the NASA standard specimen illustrated in Figure 8.

Figures 9, 10 and 11 show the relation between the notched tensile strength ratio and tensile strength. It is clearly seen that vacuum-melted material has higher tension ratio than the air-melted material.

3) ASTM notch tension test

High strength material such as maraging steel occasionally fails with unstable fracture at the stress level below its yield stress.

To evaluate this property, ASTM notch tension tests using a specimen illustrated in Figure 12 were carried out and the stress intensity factor (Kc) was calculated.

Kc value was given by equations (1) and (2). Notch in M steel specimen is the fatigue notch but in other steels the 0.1 mm radius machine cut notch were prepared.

(a) Center notch tension test

$$\begin{aligned} K_c &= \sigma w q_1(u) \\ q_1(u) &= \tan u \\ u &= \frac{\pi a}{w} + \frac{K^2}{2w\sigma_y^2} \end{aligned} \qquad (1)$$

(b) Edge notch tension test

$$\begin{aligned} K_c &= \sigma w q_2(u) \\ q_2(u) &= \tan u + 0.1 \sin 2u \\ u &= \frac{\pi a}{w} + \frac{K^2}{2w\sigma_y^2} \end{aligned} \qquad (2)$$

where

σ; Gross section stress at first fracture
σ_y; 0.2 per cent offset tensile yield strength
w; Specimen width
a; Half crack length at final unstable fracture.

In equations (1) and (2), $q_1(u)$ and $q_2(u)$ are read on interpolation line through points $(\sigma/\sigma_y)^2$, $(\pi a/w)$.

The results of ASTM notch tension tests are shown in Table 5. From these

Table 5-1. Results of the ASTM notch tension test

Steel	Aging temperature (°C)	Dimension of Specimen (mm) Thickness t	Width W	Notch length 2a	Test temperature (°C)	Fracture load (Kg)	Stress (Kg/mm²) σ_N	σ_G	$q_{1,2}$	$\sqrt{qW}$	Kc (Kg$\sqrt{\text{mm}}$/mm²)
A	480	1.00	22.00	5.96	15	2,370	147.8	107.7	.528	3.41	366
		1.02	22.00	5.90		2,320	144.1	103.4	.522	3.39	350
		1.02	22.05	6.06		2,300	143.8	102.3	.536	3.44	352
		1.04	22.00	5.96		2,380	148.4	104.0	.526	3.41	353
D	480	1.90	33.95	5.52	15	3,895	89.4	60.4	.646	4.68	282
		1.87	34.05	5.54		4,190	97.5	65.7	.648	4.69	308
		1.78	33.95	5.54		3,500	86.0	58.0	.648	4.68	271
		1.83	33.95	5.54		4,075	97.9	65.6	.648	4.68	307
E-1	430	6.25	100.00	35.7	17	17,250	43.0	27.6	.720	8.21	234
		6.18	100.00	35.7		26,800	67.4	43.4	.720	8.21	368
	480	6.27	100.00	35.7	17	22,200	55.1	35.4	.718	8.46	299
		6.26	100.00	35.7		25,300	63.0	40.6	.718	8.46	343
	550	6.13	100.00	35.8	17	21,250	54.1	34.6	.718	8.46	293
		6.16	100.00	35.8		21,250	53.8	34.4	.718	8.46	291
E-2	480	4.91	100.00	33.7	25	23,200	71.4	47.3	.585	7.65	362
		5.02	100.00	34.0	−75	21,000	63.5	41.9	.591	7.69	322
		5.01	100.00	33.5		20,550	61.6	41.0	.581	7.62	312
		5.03	100.00	33.9	−196	15,950	47.9	31.7	.589	7.67	243
		5.02	100.00	33.9		14,750	44.3	29.3	.589	7.67	225
F	440	4.99	100.00	35.7	17	34,150	106.1	68.7	.717	8.46	580
	460	5.01	100.00	35.7		28,600	88.7	57.0	.713	8.44	480
	480	4.96	100.00	35.7		24,050	75.4	48.5	.713	8.44	409
G	420	5.01	100.00	35.9	17	29,600	92.0	59.1	.723	8.50	502
	440	5.01	100.00	35.9		28,500	88.7	56.8	.723	8.50	483
	460	4.97	100.00	35.9		25,300	79.4	50.9	.723	8.50	432
	480	4.97	100.00	36.0		22,400	70.4	45.1	.723	8.51	384
H	480	5.07	100.00	34.5	19	43,300	129.3	85.4	.602	7.76	663
		5.06	100.00	34.5		42,830	129.9	84.6	.602	7.76	657
		5.06	100.00	34.5		42,900	129.7	84.9	.589	7.67	652

A, D, E-1, F and G steel specimens are side-notch specimen and other specimens are center-notch specimen.

The notch of specimens are machine cut notch.

results, the Kc values are plotted in Figure 13. It is known from Figure 13 that the Kc value and tensile strength have a linear relationship and it is represented by equation (3).

Further, it is seen from the figure that vacuum melted material has a better fracture toughness than air melted material.

Table 5-2. Results of the ASTM notch tension test

Steel	Aging temperature (°C)	Dimension of specimen: Thickness t	Width W	Notch length 2a	Test temperature (°C)	Fracture load (Kg)	Stress (Kg/mm²): σ_N	σ_G	$q_{1,2}$	$\sqrt{qW}$	Kc (Kg $\sqrt{mm}$ /mm²)
I	450	5.01	100.00	33.6	18	35,200	106.0	70.4	.583	7.64	538
		5.00	100.00	33.8		38,300	116.0	76.6	.588	7.66	586
		5.00	100.00	34.5		36,200	110.3	72.4	.600	7.75	561
J	440	5.02	100.00	34.1	18	42,000	126.5	83.7	.591	7.70	644
		4.99	100.00	33.6		40,400	121.5	80.8	.583	7.64	617
		4.96	100.00	33.7		41,000	124.3	82.7	.585	7.65	633
	480	5.00	100.00	33.8	25	29,900	90.4	59,9	.587	7.66	459
		4.99	100.00	33.8		31,400	95.1	62.9	.587	7.66	481
		5.03	100.00	34.4	−75	26,450	80.3	52.6	.600	7.75	407
		5.02	100.00	34.4		24,150	73.8	48.1	.600	7.75	393
		5.03	100.00	34.1	−196	21,750	65.7	43.2	.593	7.70	332
		5.02	100.00	33.7		16,300	49.0	32.5	.585	7.65	249
K	450	5.01	100.00	33.9	18	22,000	67.6	44.0	.589	7.67	338
		5.00	100.00	33.9		22,000	67.6	44.4	.589	7.67	340
		5.01	100.00	33.9		21,900	66.6	43.8	.589	7.67	336
L	480	5.00	100.00	34.7	18	28,900	87.3	58.8	.605	7.77	457
		5.01	100.00	34.5		26,300	79.8	52.6	.602	7.76	409
		5.01	100.00	34.3		29,500	89.1	59.0	.600	7.75	457
M	480	5.01	99.91	56.8	32	19,900	65.9	39.8	1.328	11.51	458
		4.93	99.95	54.1		27,550	85.5	55.9	1.299	11.39	637
		5.11	99.91	55.3		24,150	74.5	47.3	1.297	11.38	538

I, J, K, L and M steel specimens are center notch specimen.
I, J, K and L steel specimens have machine cut notch and M steel specimen has fatigue notch.

$$K_c = A - B\,\sigma_B \qquad (3)$$

where

A, B; Constants depending on material
σ_B; Tensile strength

In the presence of a sharp crack in a very wide (infinite) plate, the Kc value is related with the applied critcial stress (σ_c) at unstable fracture by the following formula,

$$K_c = \sigma\sqrt{\pi a} \qquad (4)$$

where

$2a$ = Crack length.

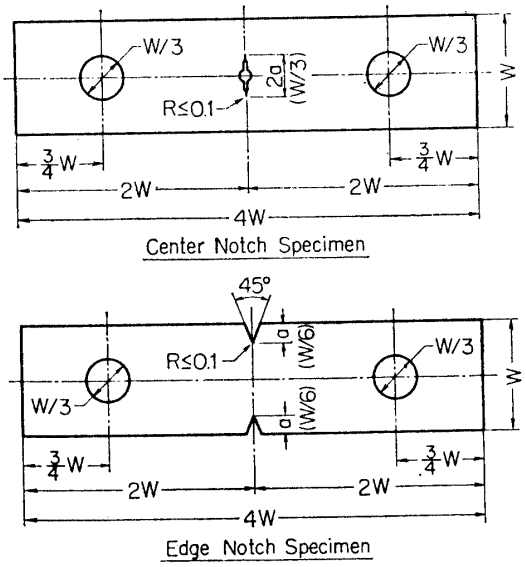

FIG. 12. Specimen of ASTM notch tension test.

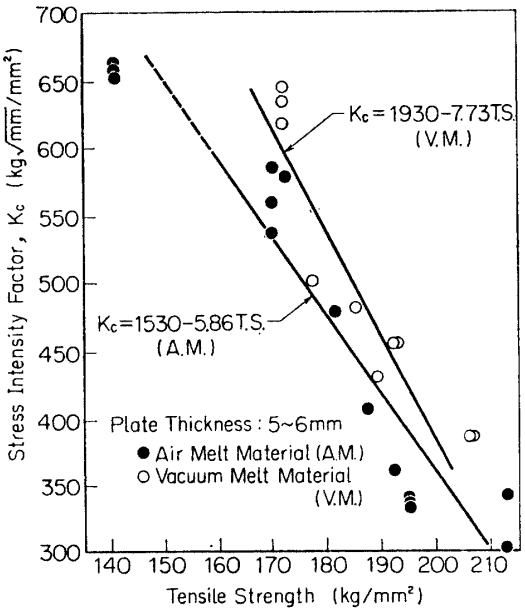

FIG. 13. Tensile strength vs. stress intensity factor (Kc).

Assuming an applied stress to be 1/1.6 of tensile strength, the critical crack length can be calculated from equations (3) and (4).

4) Surface notch tension test

It is natural to consider that actual unstable fracture of a welded structure such as a rocket motor case would be caused with higher probability from micro defect in material or surface defect than from thickness crack.

The stress intensity factor (K_{Ic}) was calculated from equation (5), where the surface notch tension test specimen illustrated in Figure 14 were used.

$$K_{Ic}=\sqrt{\frac{1.2\pi\sigma^2 a_0}{\Phi^2-0.212(\sigma/\sigma_y)^2}}$$

$$\Phi=\int_0^{\pi/2}\sqrt{1-\frac{C_0^2-a_0^2}{C_0^2}}\sin^2\theta\,d\theta \qquad (5)$$

where

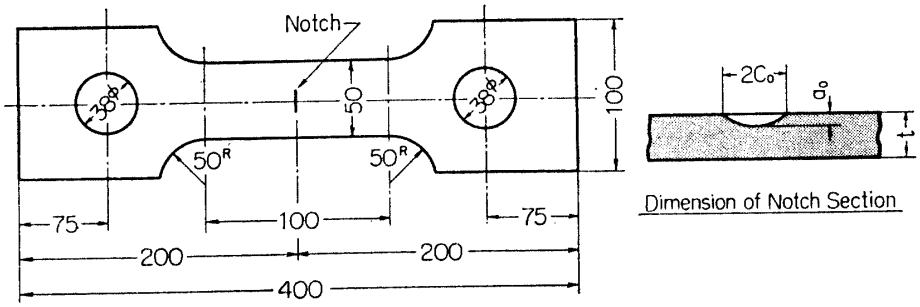

FIG. 14. Specimen of surface notch tension test.

σ: Gross section stress at fracture initiation
σ_y: 0.2 per cent offset tensile yield strength
Φ: Notch "Shape" factor in the form of an elliptical intergral function of a_0/C_0
a_0: Depth of surface notch
C_0: Half length of surface notch

The notch on M steel specimen has the fatigue-cracked notch tip but the notch of E-2 steel specimen is machined.

The results of the surface notch tension test are shown in Table 6.

Table 6. Results of the surface notch tension test

Steel	Aging temperature (°C)	Dimension of specimen (mm)				Test temperature (°C)	Fracture load P (Kg)	Stress (Kg/mm²)		K_{IC} (Kg $\sqrt{mm}$ /mm²)
		Thickness t	Width W	Notch depth a_0	Notch length $2C_0$			σ_N	σ_G	
E-2	480	5.02	50.01	2.5	15.7	17	28,400	123.3	113.0	317
		4.97	49.97	1.9	14.1		29,750	128.0	120.0	296
		4.97	50.05	2.0	15.5		32,000	142.4	128.8	328
		5.01	50.03	2.2	15.1	−75	33,000	142.7	132.0	347
		4.97	50.02	2.0	15.9		28,050	127.1	113.0	289
		5.02	50.02	2.4	15.7	−196	24,350	106.3	103.0	266
		5.04	49.97	1.9	14.2		22,450	95.4	89.3	221
		4.99	50.04	1.9	15.4		30,000	132.8	120.0	300
M	480	4.98	24.92	2.4	8.6	28	15,480	143.5	124.7	314
		4.95	24.88	1.8	6.0		19,650	171.4	159.6	345

E-2 steel specimen has machine cut notch and other specimens have fatigue notch.

3. Weld Metal Properties

3-1 Welding process

Welding processes for maraging steels that have been adopted include the MIG welding, submerged arc welding and TIG welding. Where welds of high quality are required, as in rocket motor cases, the TIG welding process is seen to be most suitable.

Consequently, welding in our case has been done with manual or automatic TIG welding using a filler metal similar to the base metal.

Further, unlike the usual high strength steel of low alloy type, a welding crack did not occur even when pre-heat or post heat operations were not done in this steel.

Therefore, it seems desirable to use an interpass temperature of as low as possible from the viewpoint of preventing the enlargement of the size of the bond grain.

Some results of tensile test of welded joints of maraging steel are shown in

Table 7. Results of the tensile test for welded joint.

Steel	Welding process	Heat treatment[1]	Tensile strength (Kg/mm²)	Elongation (%)	Fracture zone
A	Manual TIG Welding	W→480°C×3 hrs A.C.	189.4		Deposited metal
			189.4		Deposited metal
			190.9		Deposited metal
		W→S→480°C×3 hrs A.C.	196.4		Bond
			199.4		Bond
			198.1		Bond
D	Automatic TIG Welding	W→S→480°C×3 hrs A.C.	195.0	2.5[2]	Deposited metal
			195.4	1.5	Deposited metal
E-1	Automatic TIG Welding	W→480°C×3 hrs A.C.	192.1	4.0[2]	Deposited metal
			195.5	5.5	Deposited metal
		W→S→480°C×3 hrs A.C.	200.5	4.0[2]	Bond
			201.1	3.5	Deposited metal
F	Automatic TIG Welding	W→S→480°C×3 hrs A.C.	184.8	7.5[2]	Deposited metal
			183.7	6.0	Deposited metal
G	Automatic TIG Welding	W→480°C×3 hrs A.C.	186.2	3.0[4]	Soft zone
			188.7	3.5	Soft zone
		W→S→480°C×3 hrs A.C.	196.6	7.0[3]	Deposited metal
			191.1	5.6	Deposited metal
H	Automatic TIG Welding	W→S→480°C×3 hrs A.C.	151.6	16.0[3]	Bond
			151.0	17.2	Bond
I	Automatic TIG Welding	W→S→450°C×3 hrs A.C.	158.7	12.8[3]	Deposited metal
			159.1	12.8	Deposited metal
J	Automatic TIG Welding	W→S→440°C×3 hrs A.C.	165.7	11.2[3]	Deposited metal
			165.9	14.0	Deposited metal
K	Automatic TIG Welding	W→S→450°C×3 hrs A.C.	183.4	6.4[4]	Deposited metal
			183.3	8.4	Deposited metal
L	Automatic TIG Welding	W→S→480°C×3 hrs A.C.	194.6	8.4[4]	Bond
			196.5	8.4	Bond

1) W: Weld, S: 820°C×1 hr A.C.
2) GL=20 mm
3) GL=30 mm
4) GL=50 mm

Table 7.

Strength of the welded joint seems to increase when solution process is added before aging process. This trend seems to be due to softening of the heat affcted zone.

Ductility of deposited metal is shown in Table 8. The general elongation (a) is shorter than that of the base metal listed in Table 4.

Table 8. Results of ductility test for deposited metal

Steel	Strength (Kg/mm²)		General elongation (%)
	Yield	Tensile	
H	138.8	146.1	2.59
I	154.4	162.4	0.667
J	141.2	146.9	0.614
K	169.8	177.4	0.523
L	182.5	186.6	0.278

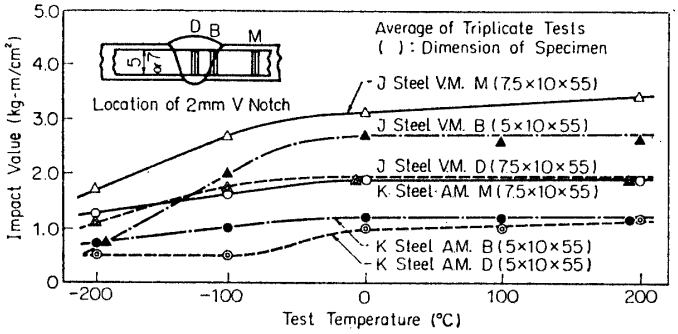

FIG. 15. Charpy transition curves of weldment for precipitation hardenable high strength steel.

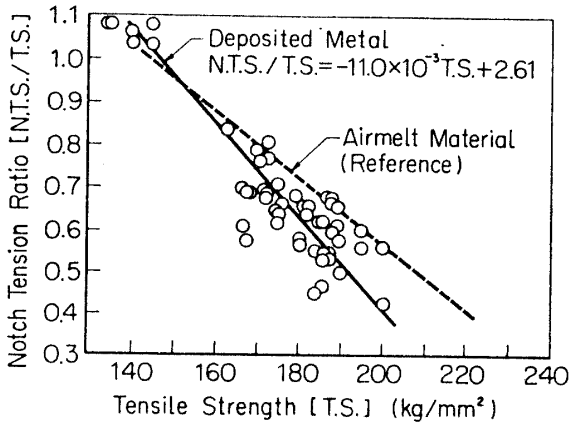

FIG. 16. Results of NASA notch tension test of deposited metal.

3-3 Fracture toughness

Various fracture toughness tests were done for the deposited metal, similarly with the base metal.

1) Charpy impact test

Figure 15 shows some measured Charpy transition curves on the specimen with a 2 mm V notch.

Table 9. Results of the ASTM notch tension test for deposited metal

Steel	Heat treatment	Dimension of specimen (mm) Thickness t	Width W	Notch length 2a	Test temperature (°C)	Fracture load (Kg)	Stress (Kg/mm²) σ_N	σ_G	$q_{1,2}$	$\sqrt{qW}$	Kc (Kg$\sqrt{\text{mm}}$/mm²)
A	W[1)]→A[3)]	1.03	30.05	5.9	15	3,590	144.0	116.0	.374	3.35	389
		1.02	30.00	5.8		3,010	125.0	98.4	.370	3.33	327
		1.07	22.00	5.9		1,730	100.0	73.5	.522	3.39	249
D	W→S[2)]→A	1.68	34.00	5.8	15	2,625	69.8	46.0	.529	4.24	195
		1.82	34.00	5.8		3.730	91.6	60.3	.529	4.24	255
		1.83	34.00	5.8		3,445	84.2	55.4	.529	4.24	234
		1.87	34.00	5.8		3,655	87.4	57.5	.529	4.24	244
E-1	W→S→A	6.51	99.75	35.6	16	17,200	41.0	32.0	.664	8.14	216
		6.31	99.75	35.7		15,500	38.3	29.4	.674	8.20	202
		6.34	99.75	35.6		19,200	47.0	32.2	.664	8.14	246
H	W→S→A	5.05	100.00	33.8	16	44,500	133.1	88.2	.588	7.66	676
		4.91	100.00	34.2		41,800	129.5	85.1	.594	7.71	657
I	W→S→A	5.00	100.00	34.5	16	22,000	66.9	44.0	.600	7.75	341
		4.98	100.00	34.0		21,000	63.8	42.2	.591	7.69	326
		5.00	100.00	34.2		27,000	81.6	54.0	.593	7.70	416
J	W→S→A	4.98	100.00	34.0	16	29,000	88.4	58.2	.591	7.69	447
		5.00	100.00	34.2		30,400	92.6	60.8	.593	7.70	468
		4.95	100.00	34.2		22,000	67.9	44.4	.593	7.70	342
K	W→S→A	5.01	100.00	34.4	16	16,500	49.8	33.0	.600	7.75	256
		5.01	100.00	34.7		15,700	47.9	31.4	.605	7.78	244
		5.00	100.00	34.5		16,400	50.0	32.8	.600	7.75	254
L	W→S→A	5.01	100.00	34.1	16	16,000	48.4	32.0	.593	7.75	246
		5.01	100.00	34.3		14,700	44.9	29.4	.596	7.71	227
		5.01	100.00	34.0		16,100	49.1	32.2	.589	7.67	247
M	W→S→A	5·01	99.77	48.3	32	14,250	44.5	28.5	.974	9.85	281
		5.00	99.78	49.2		13,100	41.8	26.3	.997	9.98	262
		5.00	99.80	50.6		13,000	41.5	26.1	1.045	10.21	266

1) Weld 2) Solution treatment 3) Aging treatment

A, D and E-1 steel specimens are Side notch specimens and other specimens are center notch specimen.

M steel specimen has fatigue notch and other steel specimens have machine cut notch.

The toughness values are a little lower than those of the base metal.

2) NASA notch tension test

The NASA notch tension tests were performed in a similar manner to those of the base metal. Ratio of notch tensile strength to tensile strength of the deposited metal is shown and compared with that of the base metal in Figure 16.

Table 10. Results of the surface notch tension test for deposited metal of M steel

Steel	Heat treatment	Dimension of Specimen (mm)				Test temperature (°C)	Fracture load (Kg)	Stress (Kg/mm²)		K_{IC} (Kg $\sqrt{mm}$ /mm²)
		Thickness t	Width W	Notch depth a_0	Notch length $2C_0$			σ_N	σ_G	
M	W→S→A	5.01	24.98	2.0	6.4	23	9,400	81.7	75.1	162
		5.02	24.89	2.1	7.0		10,200	89.9	81.6	183
		4.97	24.90	2.1	6.2		10,650	93.8	86.1	185

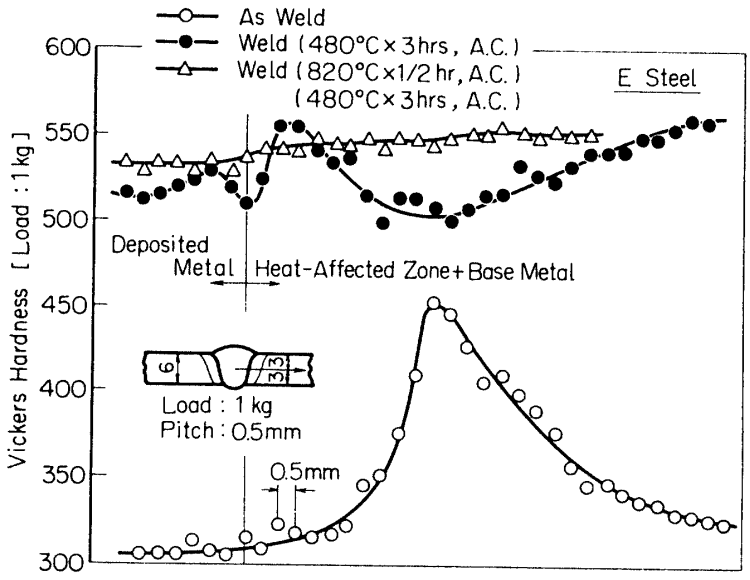

FIG. 17. Distribution of hardness of weldment for E steel.

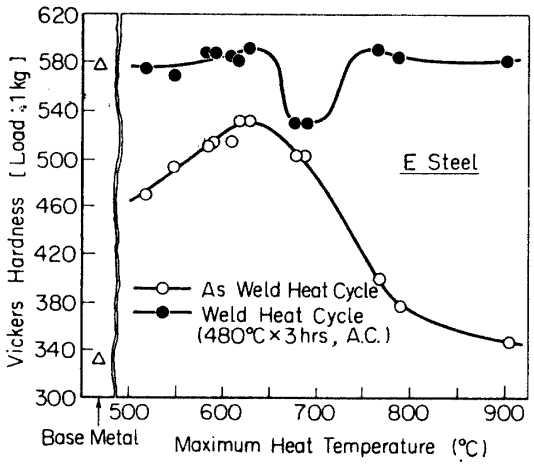

FIG. 18. Maximum heat temperature on simulated weld heat cycle vs. Vickers hardness.

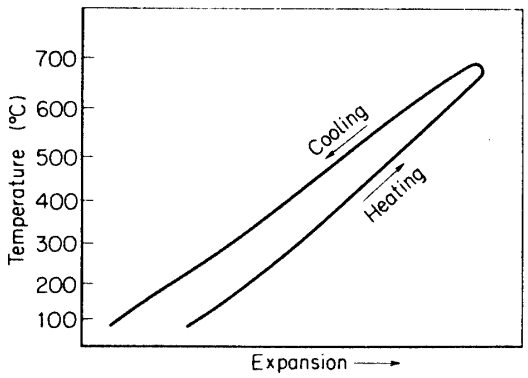

FIG. 19. Heat expansion vs. temperature in simulated test of heat affected zone (maximum heat temperature: 690°C).

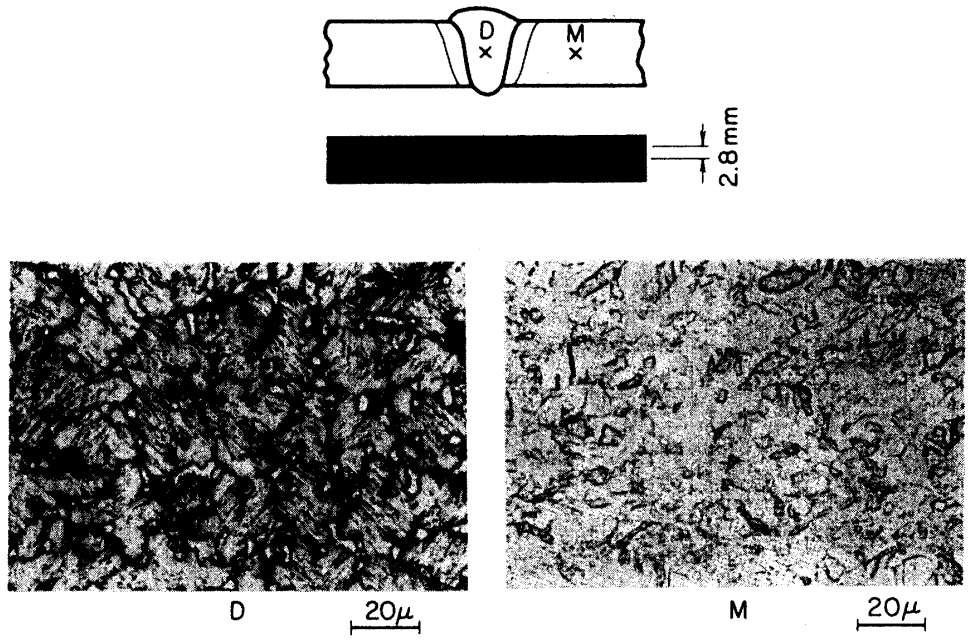

FIG. 20. Typical macro and micro structure.

It can be seen that toughness of deposited metal is considerably lower than that of base metal when the tensile strength is high.

3) ASTM notch tension test

Results of ASTM notch tension tests of deposited metals are shown in Table 9.

4) Surface notch tension test

As shown in Table 10, the K_{Ic} value of deposited metal of M steel obtained with surface fatigue notch specimen, is nearly half of the base metal.

3-4 Distribution of hardness of weldment

Figure 17 shows the hardness of weldment, which shows that the aging treatment carried out after welding process produces a soft heat-affected zone.

To investigate this phenomena further, welding thermal cycles with various maximum temperatures were applied to small specimens employing a high frequency induction furnace, and hardness of these specimens with or without aging treatment was observed. The result is shown in Figure 18, from which it is clear that the specimen heated to 640–740° are soft.

Thermal expansion of the metal under heating and cooling cycle with maximum temperature of 690°C is shown in Figure 19. As is clear from this figure, the transformation $\alpha \rightarrow \gamma$ forms a stable austenite structure which is directly cooled to the room temperature, so that it does not harden even when an aging treatment is performed.

This type of soft zone disappears completely by applying a solution treatment after welding; hence it seems desirable to perform a solution treatment when the structure requires a welded joint of high efficiency.

3-5 Macro and micro structure of welded joints

Macro and micro structure of welded joints are shown in Figure 20.

4. Burst Test of Small Models

After evaluation of the metal and welding process, steps proceeded to burst test of the vessel. To investigate the adequacy of material and the fabrication process for the rocket motor cases, small model cases were fabricated and a hydraulic pressure was applied until burst.

4-1 Shape of model case

Dimensions of a small model case are shown in Figure 21. The case is a

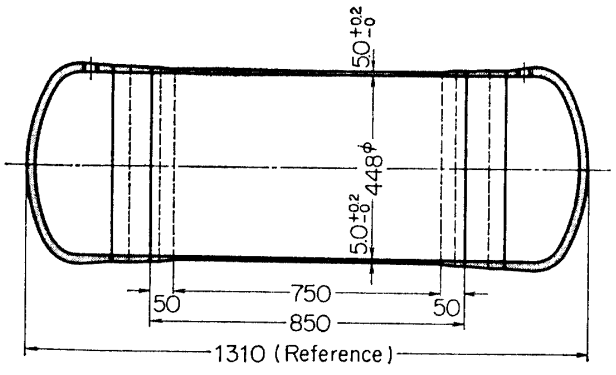

FIG. 21. Dimensions of model vessel.

Table 11. Results of fracture test for model vessel

Steel	Melting process	Tensile strength of base metal (Kg/mm²)	Dimension of model vessel (mm)				Pressure at fracture P (Kg/cm²)	Fracture zone	Fracture stress σ (Kg/cm²)	Effective fracture stress $\bar{\sigma}$, (Kg/mm²)	K_{IC} (Kg $\sqrt{mm}$ /mm²)	Remark
			Thickness t	Inner diameter D	Notch depth a_0	Notch length $2C_0$						
A	A.M.	200	3.10	400	—	—	260	Soft zone	167.7	148.9	—	W[2]→A
			3.20	426	—	—	215	Weld	143.1	125.8	—	
B	V.M.	201	3.06	426	—	—	150	Weld	104.4	91.3	—	
E-2	A.M.	185	6.56	447	—	—	340	Weld	115.8	76.4	—	W→S[3]→A[4]
			6.32	448	2.0	48.5	275	Notch	97.4(142.5)[1]	—	271	
H	A.M.	141	5.5	448	—	—	380	Base metal	155.0	136.2	—	
I	A.M.	170	5.6	448	—	—	475	Base metal	190.0	167.0	—	
J	V.M.	172	5.3	448	—	—	480	Base metal	204.0	180.2	—	
K	A.M.	195	5.3	448	—	—	480	Weld	204.0	180.2	—	
L	V.M.	191	5.7	448	—	—	540	Weld	216.0	190.8	—	
			5.64	448	2.0	49.7	290	Notch	115.2(178.3)[1]	—	329	

1) True fracture stress 2) Weld 3) Solution treatment 4) Aging treatment

cylinder with welded end plates, with a diameter of 448 mm and a length of 750–900 mm.

To investigate the fracture characteristics of the vessel, an artificial notch was cut at the base metal surface of the shell and the effect of the notch at rupture was examined comparing with that of the flat sheet test specimen.

4-2 Procedures of burst test

Before the burst test, thickness of the vessel plate is measured by ultrasonic thickness meter, and the surface of the vessel was marked with 50 mm × 25 mm stripes in order to measure deformation of the vessel plate at rupture.

Hydrostatic pressure inside the vessel is increased with increments of 5 or 10 kg/cm^2 and the strains at many parts were measured by wire strain gauges.

4-3 Test results (Table 11)

The fracture stress (σ) and the effective fracture stress ($\bar{\sigma}$) in this Table are given by equations (6) and (7).

$$\sigma = \frac{PD_0}{2T_0} \tag{6}$$

$$\bar{\sigma} = \frac{\sqrt{3}}{2} \cdot \frac{PD}{2T_0}(1 + 2\varepsilon_{0y} + \varepsilon_{0x}) \tag{7}$$

where

P: Pressure at fracture
D_0: Initial inner diameter
T_0: Initial plate thickness
ε_{0x}: Measured axial strain
ε_{0y}: Measured circumferential strain

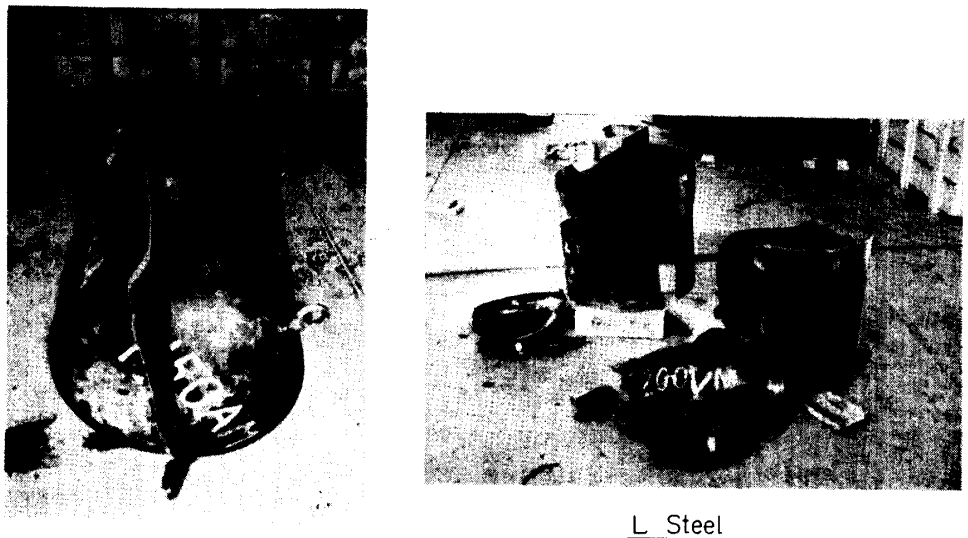

H Steel L Steel

FIG. 22. Some examples of the fracture appearance of rocket chamber models.

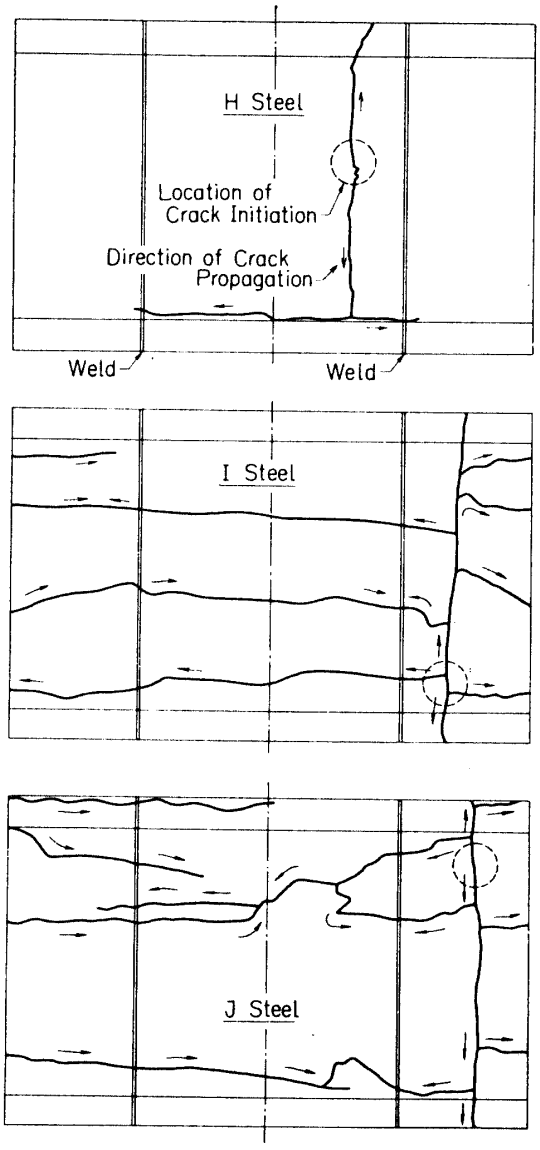

FIG. 23. Deployed view of fracture part of rocket chamber models.

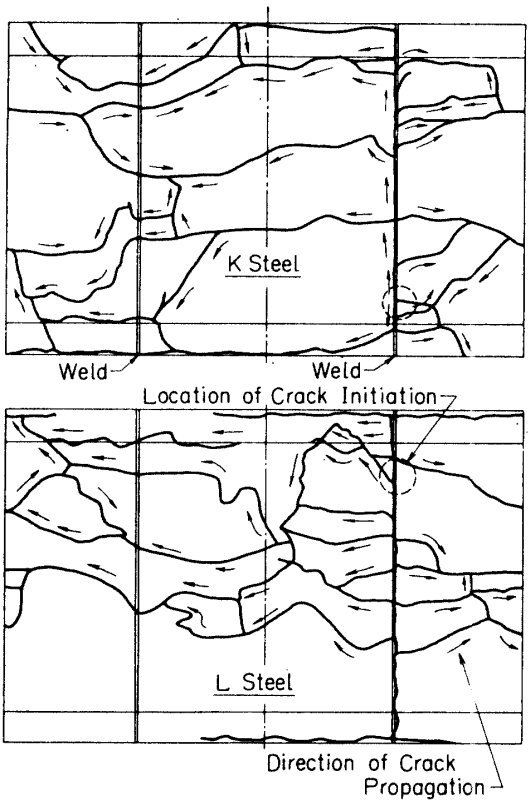

FIG. 24. Deployed view of fracture part of rocket chamber models.

K_{Ic} was calculated by equation (5), where the effect of the curvature of the cylindrical vessel was not taken in consideration. However, the obtained value is nearly equal to that of the flat sheet tensile specimen.

Figure 22 are photographs of the burst test models. Figures 23 and 24 show a deployed view of the failed part of the models.

As shown in Figure 25, the fracture stress is not equal to tensile strength of the base metal.

The fracture stress is dependent on many factors such as strength level, solution treatment, working process or welding process.

As for the relation between the fracture stress and tensile strength, the fracture stress without unstable fracture is generally higher than the tensile strength. But, as can be seen in Figure 26, actual fracture in our cases occurred at almost the

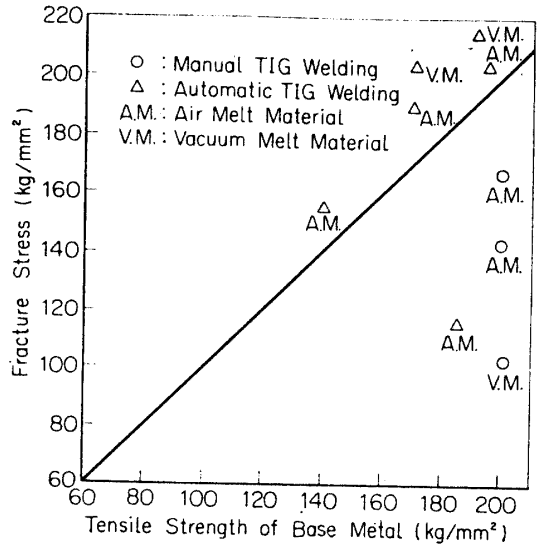

FIG. 25. Tensile strength of base metal vs. fracture stress.

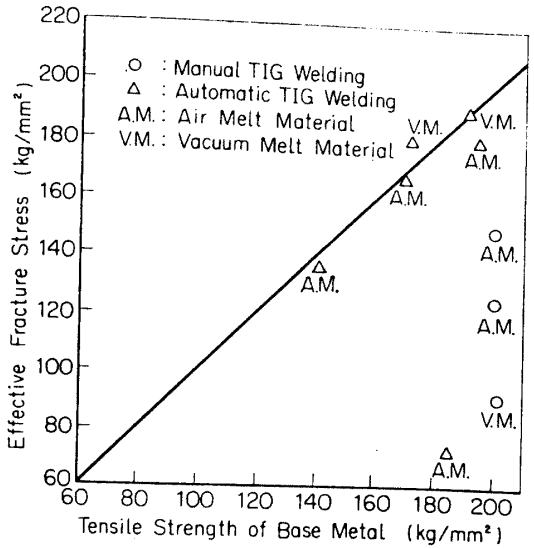

FIG. 26. Tensile strength of base metal vs. effective fracture stress.

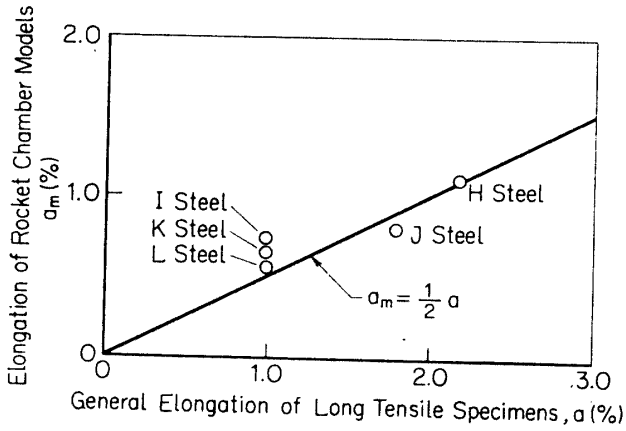

FIG. 27. General elongation of long tensile specimens vs. elongation of rocket chamber models.

same stress level as the tensile strength.

Next, the relation between elongation in the circumferential direction of the vessel after the burst test and the general elongation of the long tensile specimen is shown in Figure 27. The effective strain at the maximum load of the thin cylindrical vessel corresponds to 1/2 of the strain at the maximum load in the tensile test.

In this test, this relation is approximately the same. The fracture mode is a 45° ductile fracture at the strength level of 150 kg/mm² (H steel) and as the strength level goes up, the mode of fracture becomes more brittle.

Electron microscope fractographs (Figure 28) at the location of crack initiation in the E steel (200 kg/mm² class air melted steel) shows complete grain boundary cracks, very similar to cases where stress corrosion or hydrogen cracks grow.

Also, at the location of crack propagation, some partial quasi-cleavage of plastic deformation is seen.

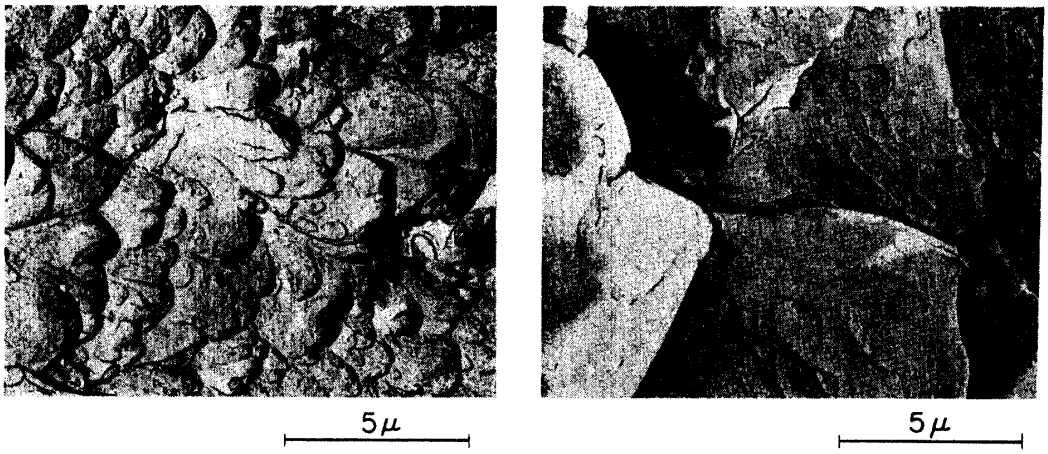

FIG. 28. Electron microscope fractogaphs of rocket chamber model (E-2 steel).

5. FABRICATION OF ACTUAL ROCKET MOTOR CASES

The application of PH 200 to actual rockets was started with the third stage motor cases of Lambda 3 rocket and Lambda 3H rocket, as previously mentioned.

Following these applications and the many research works described so far, the first stage motor case for Mu rocket was fabricated in 1965.

This motor case is a cylinder with a diameter of 1400 mm and 10 meters in length and is shown in Figure 29. When loaded with propellant, its weight is abuot 25 tons and so it cannot be transported by railway or trucks from the factory to the rocket range.

Therefore, the engine with propellant is fabricated in three segments and after transportation to the range, they are joined together. The case is bolt-joined at the flange and the propellant is bonded together by adhesives.

As can be seen in Figure 29, the length of each segment is about 3.5 m.

This motor case was used for the static firing test of Mu first stage engine at Noshiro Testing Center of the University of Tokyo in 1965. Following the static test, the flight test of M-1-1, with the first stage alone loaded with propellant, was carried out in October 1966 at the Kagoshima Space Center of the University of Tokyo.

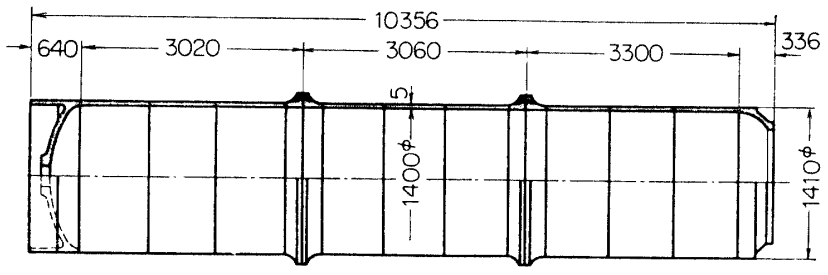

FIG. 29. The sketch of the first stage engine case of Mu rocket.

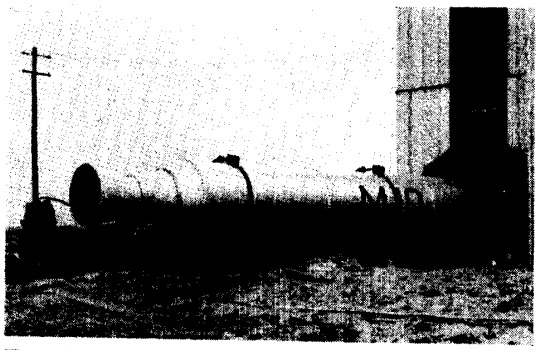

FIG. 30. Mu rocket engine for the ground static test.

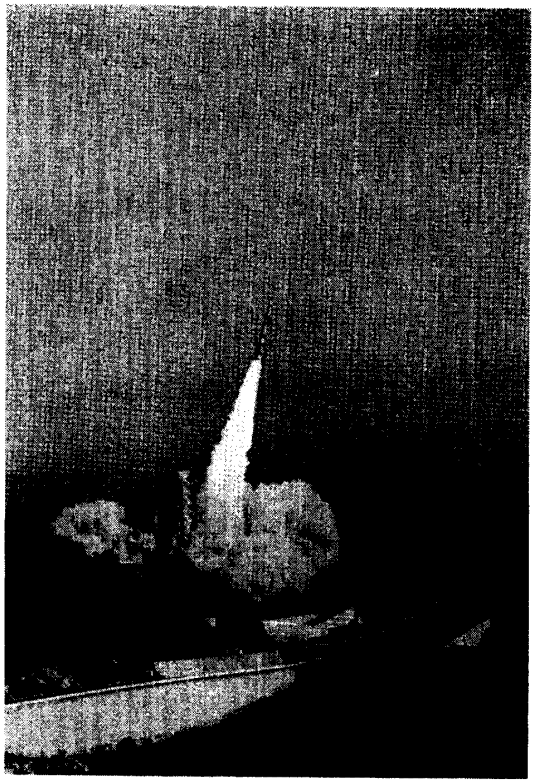

FIG. 31. Flight of M-1-1 rocket.

Both tests were quite successful. Figure 30 shows the general view of Mu first stage engine for the static test, and Figure 31 shows the launching of M-1-1.

Since then, other three Mu have been fired, i.e. M-3D-1 in 1964, M-4S-1 in 1965 and M-4S-2 in 1966. M-4S-2 has succeeded in putting the technology satellite MS-T1 in earth orbit.

In the M-4S rocket, PH 200 is used on the motors of the first three stages. The diameter of the first and second stages are 1400 mm, and the diameter of the third stage is 860 mm. Thus, PH 200 played an important role in the build up of the M-4S project.

ACKNOWLEDGEMENT

The authors must express their sincere thanks to those who contributed so much to the completion of our PH 200 motor cases, both in the research and fabrication fields.

Department of Space Technology
Institute of Space and Aeronautical Science
University of Tokyo
May 20, 1971

References

[1] Yoshio Ando; "Application of High Strength Materials for Rocket Motor Cases", Public Session Paper III-2, IIW Kyoto, 1969.

[2] Yoshio Ando, Daikichiro Mori and Kazuhisa Suzuki: "Development of Rocket Motor Case in Japan", Proc. 6th ISTS, 1965.

[3] Carl E. Hartbower: "The Role of Weld Fracture Toughness in the Performance of a 260-In.-Dia Rocket Motor Case", Public Session Paper III-1, IIW Kyoto, 1969.